Synthesis, *In Vitro* Skin Permeation Studies, and PLS-Analysis of New Naproxen Derivatives[1]

Horst Weber,[2,5] Uta Steimer,[2] Raimund Mannhold,[3] and Gabriele Cruciani[4]

Received February 1, 2001; accepted February 12, 2001

Purpose. To synthesize new naproxen (**01**) derivatives with amide or ester structures or with a combination of the two (**02–15**). To compare their physicochemical properties with naproxen esters (**16–22**) and their respective skin permeation behavior. To study structure-permeation relationships via partial least squares (PLS)-analysis.
Methods. Stability, aqueous, and octanol solubility were determined. Lipophilicity and further 53 chemical descriptors were computed. A suitable *in-vitro* skin permeation model was developed to compare maximal flux (J_{max}) of derivatives. Based on these flux data, PLS-analysis was performed to derive structure-permeation relationships.
Results. None of the new derivatives showed an improved flux in comparison to naproxen. This result can be explained by PLS-analysis: skin permeation increases with the solubility both in water and in octanol. For a good permeation, an optimized molecule should exhibit a small volume with a spherical shape. The surface area should be large in relation to volume, as indicated by the rugosity parameter. A clear separation between the hydrophobic and the hydrophilic domain (= high amphiphilic moment) is favorable. Lipophilicity is inversely correlated with skin permeation.
Conclusions. PLS-analysis is a valuable tool to derive significant, internally predictive quantitative models for structure-permeation relationships of naproxen derivatives in the above described skin permeation assay.

KEY WORDS: naproxen derivatives; synthesis; skin permeation; nude mice skin; partial least squares (PLS)-analysis.

INTRODUCTION

Nonsteroidal antiinflammatory drugs (NSAID) are widely used in the treatment of rheumatic diseases. Dermal application, if it is to give an advantage, requires the achievement of higher local drug levels in the adjacent tissues than those obtainable by oral administration. For this purpose the barrier function of the skin is the limiting factor because the bioavailability via percutaneous absorption is rather poor (1–4). There are two general possibilities to improve skin permeation. One way is by a formulation using optimal vehicles giving maximal partitioning of drugs into the skin or using penetration enhancers. The other way is a prodrug approach, which allows one to fine tune the physicochemical properties of drugs regarding skin permeation (5,6).

Some years ago, we investigated a series of esters of naproxen (7) and described an *in vitro* skin permeation model using excised skin of nude mice (8). Maximal fluxes (J_{max}) were determined and correlated with physicochemical properties: good solubilities both in octanol and in water were of prime importance for high fluxes, low heats of fusion and low molecular weights additionally contributed. In the meantime further naproxen derivatives have been reported with improved skin permeation in comparison to naproxen (6,9–11). However, some of these compounds were partially hydrolyzed already in the aqueous donor phase to a complex mixture of products. Cumulative amounts of naproxen intermediates and intact prodrugs were measured in the receptor phase to determine the steady state flux of total species. On the one hand this prodrug approach is suitable to improve dermal delivery of the parent drug and therefore has practical utility. On the other hand it is impossible to derive general relations between flux and physicochemical properties, if test compounds are unstable under the given assay conditions.

The present study describes synthesis of derivatives of the carboxylic acid naproxen incorporating amide and/or ester structures. These derivatives show a great variety of physicochemical properties, especially solubility in water and in octanol and log P values. Chemical stability of derivatives was investigated during permeation experiments in the donor and in the receptor phase. PLS-analysis of these compounds and a series of formerly described alkyl- and hydroxyalkyl-esters of naproxen (7) is presented. Physicochemical descriptors which favor skin permeation are described.

MATERIALS AND METHODS

General

Melting points were calculated from DSC-diagrams (Mettler DSC 30-TC 10) with a heating range of 5°C/min and rounded to whole numbers. IR-spectra: Perkin-Elmer 1600 Series FTIR. Mass-spectra: Finnigan 4000. ^{1}H-NMR-spectra: Bruker AC 200 F (DMSO-d_6,TMS). Elemental analysis: Perkin-Elmer PE 2400; C,H,N-values were within ± 0.3% of the calculated values. Organic chemicals were purchased from Aldrich Chemical Company. Syntheses of compounds **02–15** are described below. Naproxen esters **16–22** were synthesized as described previously (7). Solvents were of analytical grade and distilled prior use. Buffer solutions: KCl/HCl-buffer pH 2.0: 250 ml KCl (0.2 M) and 65 ml HCl (0.2 M) were diluted with water to 1 l. For preparation of phosphate-buffer solutions we used mixtures of standard solutions of (a) $Na_2HPO_4 \times H_2O$ (11.87 g/l, Merck Nr. 6587) and (b) KH_2PO_4 (9.073 g/l, Merck Nr. 4857). For pH 6 buffer solution: 121 ml of (a) + 879 ml of (b) were mixed. For pH 7.2 buffer solution: 721 ml of (a) + 279 ml of (b) were mixed. HPLC-system for determination of drug concentration in the receptor phase: Waters 510 pump, Waters 490 E programmable multi wavelength detector. Column: Lichrosorb, RP-select B (5mm) 250 × 4 mm; eluent: acetonitrile/phosphate buffer pH 2.3 or methanol/water; 1 ml/min; room temperature.

[1] Dedicated to Prof. Dr. Bernhard C. Lippold on the occasion of his 60th birthday.

[2] Department of Pharmaceutical Chemistry, Heinrich-Heine-Universität Düsseldorf, Universitätsstraße 1, D-40225 Düsseldorf, Germany.
[3] Department of Lasermedicine, Molecular Drug Research Group, Heinrich-Heine Universität Düsseldorf, Universitätsstraße 1, D-40225 Düsseldorf, Germany.
[4] Dipartimento di Chimica, Laboratorio di Chemiometria, Universitá di Perugia, Via Elce di Sotto, 10, I-06123 Perugia, Italy.
[5] To whom correspondence should be addressed. (e-mail: Horst.Weber@uniduesseldorf.de)

0724-8741/01/0500-0600$19.50/0

Synthesis of Naproxen Derivatives 02–15

*N-[2-(6-Methoxy-2-naphthyl)propionyl]-L-serine (**02**)*

L-Serine (1.05 g; 0.01 mol) was dissolved in 20 ml of water containing 1.2 g (0.03 mol) NaOH. After addition of 50 ml water and 50 ml acetone, a solution of the acid chloride of naproxen (7) (2.49 g; 0.01 mol) in a minimum amount of acetone was added dropwise and the solution was stirred for 6 h at 20°C. After evaporation to half of the volume, 50 ml water and sufficient dilute HCl was added to acidify the solution. Extraction with ethyl acetate after drying with magnesium sulphate, filtration, and evaporation gave 1.77 g (56%) of a white, crystalline powder, mp. 182°C (from ethanol/diethyl ether). ^{1}H-NMR δ 1.40 (d,3H), 3.35 (s,OH), 3.67 (t,2H), 3.86 (s,3H), 3.90 (q,1H), 4.30 (dt,1H), 7.1-7.8 (m,6H), 8.15 (d,NH), 12.51 (s,COOH). IR (KBr) 3554, 3322, 2982, 2940, 2902, 1741, 1715, 1636, 1605, 1551 cm^{-1}. MS 317 (11,M), 299 (3), 255 (1), 230 (3), 185(100). Anal. ($C_{17}H_{19}NO_5$) C,H,N.

*N-[2-(6-Methoxy-2-naphthyl)propionyl]-L-threonine (**03**)*

This compound was prepared as described for **02** from naproxen acid chloride (7) and L-threonine to give 2.85 g (86%) of **03** as a white cystalline powder, mp. 179°C (from acetone/hexane). ^{1}H-NMR δ 1.07 (d,3H), 1.42 (d,3H), 3.86 (s,3H), 4.01 (q,1H), 4.24 (dd,1H), 7.1-7.8 (m,6H), 7.91 (d,NH). IR (KBr) 3546, 3314, 3056, 2982, 2938, 1734, 1710, 1635, 1606, 1557, 1501 cm^{-1}. MS 331 (6,M), 313 (2),287 (1), 269 (2), 185 (100), 170 (12), 141 (19), 115 (13). Anal. ($C_{18}H_{21}NO_5$) C,H,N.

*N,N-Diethyl-2-(6-methoxy-2-naphthyl)propionamide (**04**)*

Naproxen acid chloride (7) (2.49 g, 0.01 mol) was dissolved in 50 ml chloroform and 1.4 g (0,02 mol) diethylamine was added. After 10 h of stirring at 20°C the organic phase was washed successively with dilute HCl, NaOH, and water, dried with magnesium sulphate and evaporated. The residue was recrystallized from diethyl ether to yield 2.45 g (86%) of a white powder, mp. 79°C (lit.12 no data given). ^{1}H-NMR δ 0.92 (t,3H), 1.01 (t,3H), 1.37 (d,3H), 3.1-3.5 (m,4H), 3.88 (s,3H), 4.12 (q,1H), 7.1-7.8 (m,6H). IR (KBr) 3058, 3027, 3005, 2976, 2961, 2951, 1636, 1602, 1505 cm^{-1}. MS 285 (5,M) 256 (1), 212 (1), 185 (94), 100 (100). Anal. ($C_{18}H_{23}NO_2$), C,H,N.

*N,N-Bis-(2-hydroxyethyl)-2-(6-methoxy-2-naphthyl)propionamide (**05**)*

This compound was prepared as described for **04** with diethanolamine and obtained as 1.27 g (40%) of white crystals, mp. 97°C (from ethyl acetate/diethyl ether). ^{1}H-NMR δ 1.34 (d,3H), 3.1-3.6 (m,8H), 3.86 (s,3H), 4.27 (q,1H), 4.64 (OH), 4.86 (t,OH), 7.1-7.8 (m,6H). IR (KBr) 3362, 3057, 2968, 2929, 2870, 1606, 1505 cm^{-1}. MS 317 (8,M), 286(1), 272 (1), 228 (1), 212 (2), 185 (100). Anal. $C_{18}H_{23}NO_4$) C,H,N.

*4-[2-(6-Methoxy-2-naphthyl)propionyl]-morpholine (**06**)*

This compound was prepared as described for **04** with morpholine and was isolated as 2.84 g (95%) of white crystals, mp. 112°C (from ethyl acetate/diethyl ether). ^{1}H-NMR δ 1.37 (d,3H), 3.1-3.6 (m,8H), 3.88 (s,3H), 4.23 (q,1H), 7.1-7.8 (m,6H), IR (KBr) 3055, 3007, 2962, 2925, 2899, 1632, 1604, 1505 cm^{-1}. MS 299 (8,M), 212 (2), 185(100). Anal. ($C_{18}H_{21}NO_3$) C,H,N.

*Aminocarbonylmethyl-2-(6-methoxy-2-naphthyl)propionate (**07**)*

Naproxen (2.30 g, 0.01 mol), 1.10 g (0.011 mol) triethylamine, 1.03 g (0.011 mol) 2-chloroacetamide and 0.15 g (0.001 mol) sodium iodide were mixed in 10 ml DMF and stirred for 2 h at 90°C. After cooling, 50 ml water was added to the mixture and it was extracted three times with 50 ml ethyl acetate. The combined organic phase was washed successively with sodium thiosulphate (2%) and sodium bicarbonate (2%). After drying ($MgSO_4$) and filtration, the residue of the evaporated organic phase gave 2.13 g (74%) white crystals, mp. 145°C (from ethanol). ^{1}H-NMR δ 1.50 (d,3H); 3.87 (s,3H), 4.04 (q,1H), 4.35 (d,1H) 4.48 (d,1H), 7.1-7.8 (m,6H). IR (KBr) 3488, 3062, 2997, 2982, 2963, 1723, 1693, 1678, 1603, 1505 cm^{-1}. MS 287 (15,M), 269 (1), 229 (1), 212 (28), 185 (100). Anal. ($C_{16}H_{17}NO_4$) C,H,N.

*N,N-Diethylcarbonylmethyl-2-(6-methoxy-2-naphthyl)propionate (**08**)*

This compound was prepared according to the procedure described for **07** with 1.64 g (0.011 mol) N,N-diethylchloroacetamide (Lancaster) and gave 3.16g (92%) white crystals, mp. 93°C (from ethanol) [lit.(13) mp. 89-89,5°C, no spectroscopic data given]. ^{1}H-NMR δ 0.99 (t,3H), 1.07 (t,3H), 1.51 (d,3H), 3.1-3.3 (m,4H), 3.87 (s,3H), 4.00 (s,1H), 4.75 (dd,2H), 7.1-7.8 (m,6H). IR (KBr) 3048, 2978, 2940, 2873, 1745, 1661, 1605, 1505 cm^{-1}. MS 343 (4,M), 271 (1), 230 (1), 212 (100), 185 (56). Anal. ($C_{20}H_{25}NO_4$) C,H,N.

*N,N-Diethanolaminocarbonylmethyl-2-(6-methoxy-2-naphthyl)propionate (**09**)*

The corresponding chloroacetamide was not commercially available. It was prepared from ethyl-chloroacetate and diethanolamine at 0°C. The complete reaction to the amide was detected by IR-spectroscopy (strong absoption band at 1644 cm^{-1} instead of the ester band at 1738 cm^{-1}). Following the procedure for **07** compound **09** was obtained as 1.61 g (43%) of a white powder, mp. 117°C (from ethyl acetate/diethyl ether) [lit.(14) mp. 113–114°C, no spectroscopic data given]. ^{1}H-NMR δ 1.50 (d,3H), 3.3-3.5 (m,8H), 3.86 (s,3H), 3.99 (q,1H), 4.69 (t,OH), 4.86 (t,OH), 4.86 (dd,2H), 7.1-7.8 (m,6H). IR (KBr) 3362, 3058, 2991, 2963, 2940, 1737, 1632, 1604, 1504 cm^{-1}. MS 375 (3,M), 358 (2), 344 (5), 328 (1) 286 (2), 271 (1), 230 (3), 212 (50), 185 (100). Anal. ($C_{20}H_{25}NO_6$) C,H,N.

*Morpholinocarbonylmethyl-2-(6-methoxy-2-naphthyl)propionate (**10**)*

The ester **10** was prepared as described for **07**. The chloroacetylamide was synthesized from chloroacetyl chloride and morpholine (1:2). **10** was isolated as 3.11 g (87%) of white crystals, mp. 123°C (from ethyl acetate/diethyl ether). ^{1}H-NMR δ 1.51 (d,3H), 3.3-3.5 (m,8H), 3.87 (s,3H), 4.01 (q,1H), 4.88 (dd,2H), 7.1-7.8 (m,6H). IR (KBr) 3049, 2967, 2933, 2906, 1742, 1657, 1605, 1505 cm^{-1}. MS 357 (7,M), 270 (1), 228 (1), 212 (100), 185 (72). Anal. ($C_{20}H_{23}NO_5$) C,H,N.

*Ethyl-N-[2-(6-methoxy-2-naphthyl)propionyl]glycinate (**11**)*

Naproxen acid chloride (7) (3.73 g, 0.015 mol) was dissolved in 50 ml ethyl acetate. Ethyl glycinate hydrochloride (1.40 g, 0.01 mol) and triethylamine (1.01 g, 0.01 mol) were added slowly to the stirred suspension. After 24 h stirring at 20°C, the organic layer was washed with dilute HCl and then with sodium bicarbonate (2%). After drying ($MgSO_4$) and evaporation of the organic layer, **11** was obtained as 2.30 g (73%) of a white powder, mp. 86°C (from ethyl acetate/diethyl ether). ^{1}H-NMR δ 1.13 (t,3H), 1.42 (d, 3H) 3.6-3.8 (m,3H), 3.92 (s,3H), 4.04 (q,2H), 7.1-7.8 (m,6H), 8.42 (t,NH). IR (KBr) 3279, 3081, 2973, 2935, 1752, 1647, 1608, 1505 cm^{-1}. MS 315 (9,M), 270 (1), 242 (1), 212 (2), 185 (100). Anal. $C_{18}H_{21}NO_4$) C,H,N.

*2-Hydroxyethyl-N-[2-(6-methoxy-2-naphthyl)propionyl]glycinate (**12**)*

N-[2-(6-Methoxy-2-naphthyl)propionyl]glycine (14,15) (2.87 g, 0.01 mol) was neutralized with 1.01 g (0.01 mol) triethylamine and 0.81 g (0.01 mol) 2-chloroethanol was added. The mixture was melted at 120°C for 12 h, then reacted with ice-cold water for 1 h. After acidification with dilute sulphuric acid, the aqueous phase was extracted with diethyl ether. This extract was washed with water, dried ($MgSO_4$), filtered, and evaporated. The residue was crystallized to give 1.25 g (38%) of a white powder, mp. 109°C (from ethyl acetate/diethyl ether). ^{1}H-NMR δ 1.42 (d,3H), 3.53 (m,2H), 3.8 (m,3H), 3.86 (s,3H), 4.04 (t,2H), 4.80 (t,OH), 7.1-7.8 (m,6H), 8.42 (t,NH). IR (KBr) 3482, 3307, 3069, 2988, 2973, 1747, 1635, 1609, 1547, 1503 cm^{-1}. MS 331 (26,M), 301 (2), 270 (2) 242 (3) 212 (3), 185 (100). Anal. ($C_{18}H_{21}NO_5$) C,H,N.

*N-(N-Ethylaminocarbonylmethyl)-2-(6-methoxy-2-naphthyl)propionamide (**13**)*

Ester **11** (3.15 g, 0.01 mol) was dissolved in 20 ml of ethylamine and stirred at room temperature for 6 h. After addition of 50 ml water, the aqueous phase was extracted with diethyl ether. The organic layer was washed with dilute HCl, sodium bicarbonate, and water and dried ($MgSO_4$). After filtration and evaporation, the residue from the organic layer gave 2.23 g (71%) of a white powder, mp. 153°C (from ethyl acetate). ^{1}H-NMR δ 0.97 (t,3H), 1.41 (d,3H), 3.05 (m, 2H), 3.51-3-76 (ddd,2H), 3.82 (q,1H), 3.86 (s,3H), 7.1-7.8 (m,6H), 8.12 (t,NH). IR (KBr) 3287, 3056, 2967, 2934, 1666, 1640, 1604, 1560, 1519, 1503 cm^{-1}. MS 314 (5,M), 270 (1), 242 (1), 228 (1), 212 (70), 185 (100). Anal. ($C_{18}H_{22}N_2O_3$) C,H,N.

*2-(6-Methoxy-2-naphthyl)-N-(1H-tetrazol-5-yl)propionamide (**14**)*

Solutions of 2.49 g (0.01 mol) naproxen acid chloride (7) in 20 ml acetone and 5.15 g (0.05 mol) 5-aminotetrazole monohydrate in 50 ml water were combined and stirred at room temperature for 12 h. After evaporation of the acetone, the aqueous solution was diluted with 50 ml water and extracted with ethyl acetate. The organic layer was washed with dilute HCl, dilute NaOH, and water, dried ($MgSO_4$) and evaporated. The residue was crystallized to give 2.52 g (85%) white powder, mp. 262°C (from ethyl acetate). ^{1}H-NMR δ 1.54 (d,3H), 3.86 (s,3H), 4.12 (q,1H), 7.1-7.8 (m,6H), 12.28 (s,NH), 15.93 (s, NH). IR (KBr) 3221, 3084, 2980, 2934, 1697, 1905, 1548, 1505, cm^{-1}. MS 297 (8,M), 240 (1), 212 (100). Anal. ($C_{15}H_{15}N_5O_2$) C,H,N.

*2-(6-Methoxy-2-naphthyl)-N-(1H-1,2,4-triazol-3-yl)propionamide (**15**)*

Naproxen acid chloride (7) (2.49 g, 0.01 mol) was dissolved in 50 ml chloroform and 3.20 g (0.02 mol) 3-amino-1,2,4-triazole was added. After stirring at room temperature for 10 h the organic phase was washed with dilute HCl, dilute NaOH and water. After drying ($MgSO_4$) and evaporation of the organic phase, the residue was heated in a flask at 200°C for 3 h. After cooling and recrystallization, **15** was obtained as 1.34 g (45%) of a white powder, mp. 242°C (from ethyl acetate). ^{1}H-NMR δ 1.56 (d,3H), 3.86 (s,3H), 4.05 (q,1H), 7.1-7.8 (m,6H), 11.77 (s,NH), 13.42 (s,NH). IR (KBr) 3254, 3060, 2988, 2953, 1685, 1606, 1557, 1505 cm^{-1}. MS 296 (1,M), 267, 252, 240, 227, 212 (82), 185 (57). Anal. ($C_{16}H_{16}N_4O_2$) C,H,N.

Stability

All model compounds proved to be stable during skin permeation tests (24 h). Neither TLC-analysis of the donor phases nor HPLC-analysis of the receptor media showed any amount of free naproxen or other degradation products.

Solubility

Solubility [mol/l] of the compounds was determined by stirring a suspension of excess pulverized derivative in water (**01**: 1.4 · 10^{-4}; **02**: 3.4 · 10^{-4}; **03**: 4.7 · 10^{-4}; **04–22**: see Table I), in 20% aqueous ethanol (**01, 04–22**), in aqueous buffer at pH 7.2 (**01–03**) and in octanol (**01–15**) over a period of 24 h at 20°C ± 0.1°C (see Table I). Solubility of **01** was also determined in buffer solution pH 2 (6.1 · 10^{-5}) and pH 6 (2.1 · 10^{-3}) under the same conditions. The aqueous solutions were filtered through a 0.2 μm membrane of cellulose nitrate (Sartorius Nr. 11307). A filter of regenerated cellulose (Sartorius Nr. 11607) was used in the case of octanol. The solutions were analyzed by UV-absorption at 232 nm (water solutions) or 262 nm (octanol solutions) by means of calibration curves. Relative standard errors of the mean ($S_{rel.}$ [%]) were within ± 1% (n = 3). Solubility of **16–22** in octanol could not be measured as sufficient amounts to prepare saturated solutions were not available. Thus, these data have been calculated on the basis of solubility in water (c_w) and calculated log P values, as described previously (8). For data see Table I.

Partition Coefficients

Lipophilicities of **01–22** (Table I) were calculated with the software KOWWIN (16).

Diffusion Cell Experiments

The permeation experiments were carried out as previously described (8). Briefly, the full thickness skin of 10–14 week old female nude mice (Han: NMRI nu/nu) were prepared. The dorsal portion was fixed with the epidermal side up on Franz-type diffusion cell with a surface of 8 cm^2 and a stirred receptor volume of 49 cm^3. The experiments were carried out in an incubator at 32°C. **Donor phase**: Compounds **01–22** (0.5 g) were carefully triturated with 0.5 g of lactose.

Table I. Physicochemical and Skin Permeation Data of the Test Compounds

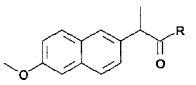

	R	log C_W[a]	log C_O	log $C_{20\%}$ EtOH	log P	$S_{rel.}$ [%]	log J_{max}
01	OH	–1.80*	–1.07	–3.39	3.10	12.3	+0.79
02	N-(L)-serin	–1.52*	–2.71	n.d.	1.31	8.5	–0.33
03	N-(L)-threonin	–1.31*	–2.09	n.d.	1.73	5.3	–1.00
04	$N\text{-}(CH_2CH_3)_2$	–3.77	–0.41	–3.05	3.88	3.5	+0.27
05	$N\text{-}(CH_2CH_2OH)_2$	–2.19	–0.75	–1.82	1.36	4.8	+0.53
06	$N\text{-}(CH_2CH_2)_2\text{-}O$	–3.14	–0.98	–2.92	2.51	1.3	+0.48
07	$OCH_2C(=O)NH_2$	–4.06	–2.35	–3.82	2.26	2.1	–0.82
08	$OCH_2C(=O)\text{-}N\text{-}(CH_2CH_3)_2$	–4.15	–1.19	–3.82	3.92	32.8	–1.00
09	$OCH_2C(=O)\text{-}N\text{-}(CH_2CH_2OH)_2$	–3.16	–2.12	–3.03	1.40	14.3	–0.39
10	$OCH_2C(=O)\text{-}N\text{-}(CH_2CH_2)_2\text{-}O$	–4.26	–2.40	–3.70	2.55	16.2	–1.69
11	$NHCH_2C(=O)OCH_2CH_3$	–3.70	–1.07	–3.29	3.22	5.3	–0.52
12	$NHCH_2C(=O)OCH_2CH_2OH$	–3.01	–1.59	–2.54	1.75	22.7	–0.34
13	$NHCH_2C(=O)NHCH_2CH_3$	–3.37	–1.52	–3.00	2.09	3.2	–0.57
14	NH-(1H)-tetrazol-5-yl	–4.70	–3.70	–4.24	1.47	34.2	–2.42
15	NH-(1H)-1,2,4-triazol-3-yl	–5.00	–3.00	–4.05	2.94	22.8	–1.39
16	OCH_3	–4.78	–1.01	–3.92	3.76	17.5	–1.10
17	OCH_2CH_3	–5.24	–0.99	–4.17	4.25	8.3	–0.85
18	$O(CH_2)_2CH_3$	–5.82	–1.08	–4.35	4.74	—	–3.00
19	$O(CH_2)_4CH_3$	–6.97	–1.24	–4.66	5.72	—	–4.00
20	$O(CH_2)_2OH$	–3.33	–0.55	–2.92	2.78	12.6	–0.27
21	$O(CH_2)_3OH$	–3.40	–0.13	–2.82	3.27	10.6	–0.21
22	$OCH_2CH(OH)CH_3$	–3.30	–0.10	–2.70	3.20	9.7	–0.43

[a] Abbreviations used: C_W = molar solubility in water or in phosphate buffer pH 7.2 (asterisked compounds), C_O = molar solubility in octanol, $C_{20\%\ EtOH}$ = molar solubility in 20% ethanol, log P = calculated lipophilicity, $S_{rel.}$ [%] = relative standard deviation of the mean value of J_{max} data [pmol/cm^2 · s]. For details see Materials and Methods.

Each of these triturations was mixed with 9.5 g of a hydroxyethyl cellulose gel, which was prepared from Tylose 1000 (2.5 g), water (77.5 g), and ethanol (20 g). It can be calculated from the solubilities of the derivatives in 20% ethanol that at least a 10fold excess of saturation of undissolved compound was present in each donor phase. These donor gels were freshly prepared and stored in the refrigerator at +4°C. **Receptor phase**: Aqueous stock solution (1l) was prepared containing $NaH_2PO_4 \times H_2O$ (0.689 g, 0.005 mol), $Na_2HPO_4 \times 2\ H_2O$ (0.889, 0.005 mol), and NaCl (87.66 g, 1.5 mol). To 100 ml of this stock solution, a solution of 150 mg of erythromycin in 5 ml of isopropanol was added and filled up with water to 1 l. If necessary, the pH of this receptor phase was adjusted to pH 7.2 with NaOH (0.01 mol/l). Permeation experiments (n = 3–5) were started with the application of 0.5 g donor gel and continued for 24 h. Concentration of the compounds (c = μg/cm^3) in the receptor phase was determined by HPLC (after filtration on glass fibre and cellulose nitrate membrane successively) using a calibration curve. Maximal flux (J_{max}) was calculated according to Eq. 1 where $\Delta m = c \cdot 49$ cm^3, $F = 8$ cm^2, and $\Delta t = 24$ h neglecting lag time:

$$J_{max} = \frac{dm}{F \cdot dt} = \frac{\Delta m}{F \cdot \Delta t} \quad [\mu g/cm^2 \cdot h] \qquad (1)$$

J_{max} data were converted to [pmol/cm^2 · s] relative standard deviations ($S_{rel.}$ [%]) and logarithms of the mean values are listed in Table I.

PLS-Analysis

Test molecules were built with the software SYBYL (version 6.5) on a Silicon Graphics workstation, SGI O2. Most physicochemical descriptors were computed from the 3D-interaction energy maps produced by GRID (17) and transformed by VolSurf (18). GRID force field detects favorable binding sites for chemical probes on the surface of target molecules: the water probe is used to define hydrophilic regions; the hydrophobic probe DRY is applied for defining hydrophobic regions. Area and volume of this envelope vary with the level of interaction energies between probe and target molecule. However, at a fixed isoenergetic contour level, the hydrophilic area and volume are well defined for each molecule. VolSurf is a program to visualize, quantify, and transform the 3D-energy maps into useful chemical descriptors. Hydrophilic and hydrophobic regions, polar and hydrophobic integy moments as well as capacity factors are computed for 8 different levels of interaction energies between the test molecule and the probe. In total 53 VolSurf descriptors were calculated in this way; for further definition of VolSurf descriptors see Table II.

Calculated lipophilicity (16) and the experimentally measured solubilities in water (log C_w) and octanol (log C_o) were used as further parameters. The logarithms of the maximal fluxes (log J_{max}) were used as permeation data. Partial least squares (PLS)-analysis (19) was performed with the GOLPE

Table II. Definition of VolSurf parameters

nr	descriptor	Information content
1	volume V	Volume ($Å^3$) contained within the water accessible surface, computed at +0.20 kcal/mol
2	surface S	Accessible surface ($Å^2$) traced out by a water probe, computed at +0.20 kcal/mol
3	volume/surface R	Measure of molecular wrinkled surface (= rugosity). The smaller the ratio, the smaller the rugosity.
4	globularity G	S/S equiv.; S equiv = surface area of a sphere of volume V. G is 1.0 for a perfect spherical molecule. Values > 1.0 for real spheroidal molecules.
5–12	hydrophilic regions W1–W8	Molecular envelope accessible by water; volume of envelope depends on level of interaction energies between water and solute. W1–W4: polarizability and dispersion forces; W5–W8: polar and HB donor and acceptor regions
13–20	polar integy moment lw1–lw8	Measure of unbalance between the center of mass of a molecule and the position of the hydrophilic regions. Polar integy moments: vectors pointing from the center of mass to the center of W1–W8.
21–28	capacity factor Cw1–Cw8	Ratio between hydrophilic regions and molecular surface; this equals the amount of hydrophilic regions per surface unit
29–31	minima distances D12, D13, D23	Distances of the best three local minima of interaction energies between the water probe and the target molecule
32–39	hydrophobic regions D1–D8	Hydrophobic regions indicate interactions with the DRY probe
40–47	hydrophobic integy moment ID1–ID8	Measure of unbalance between the center of mass of a molecule and the position of the hydrophobic regions. Hydrophobic integy moments: vectors pointing from the center of mass to the center of D1–D8.
48–49	hydrophilic/lipophilic balance HL1–HL2	Ratio between the hydrophilic regions measured at -3 and -4 kcal/mol and the hydrophobic regions measured at –0.6 and –0.8 kcal/mol. The balance describes which effect dominates in the molecule.
50	amphiphilic moment A	Vector pointing from the center of the hydrophobic domain to the center of the hydrophilic domain
51–53	interaction energy minima Emin 1–Emin 3	Energies of interaction in kcal-mol of the best three local minima of interaction energies between the water probe and the target molecule

(20) software, version 4.5.1, on a Silicon Graphics workstation.

RESULTS AND DISCUSSION

Because it is ethically impossible to test each new derivative of naproxen under *in vivo* conditions in humans it was necessary to develop a suitable *in vitro* permeation model. The results obtained in such experiments should be transferable or at least relatively applicable to *in vivo* conditions. However, the choice of either *post mortem* human skin or excised skin of various laboratory animals as a proper model to reflect *in vivo* conditions is generally problematic. Beyond the origin of the membrane there are other important factors that can profoundly effect the experimental results like effects of vehicle, dose applied to the skin, duration of exposure, and composition of donor and receptor solutions, to mention only a few.

Our aim was to ensure maximum concentration of the model compounds in the donor phase and a sufficient solubility in the receptor phase to avoid a saturated solution. Also the concentration of naproxen derivatives after permeation into the receptor phase should be sufficient to be analyzed by UV-detection after HPLC. Last but not least, the permeation model should imitate the natural barrier function of the skin as closely as possible, that is without destruction of its physiological properties.

To fulfil these requirements, we decided to use excised full thickness skins of nude mice (see Methods), representing a common *in vitro* permeation model. With regard to the formulation of donor phase and receptor phase, there are a lot of recommendations in the literature. Normally, aqueous buffer solutions containing a physiological concentration of NaCl were used, but these solutions do not sufficiently reflect the real *in vivo* conditions because not only hydrophilic but also lipophilic processes are involved during skin permeation. Aqueous ethanolic solutions have been frequently proposed as suitable receptor fluids for lipophilic compounds (21–25). As a result of a series of permeation experiments (26) with three different receptor solutions (pure aqueous buffer pH 7.2, and addition of 20% and 50% ethanol), we decided to use a 20% ethanol concentration in both donor and receptor phase. In this way, the two compartments were balanced and no concomitant flux of ethanol was associated with or against the flux of derivatives.

From 1. Fick's law the maximal flux (J_{max}) of a compound from a gel suspension is proportional to its solubility in the barrier (skin). As long as saturation of the test compounds in the vehicle (donor phase) is maintained and the compounds dissolve sufficiently fast to replace the amount permeated across the skin into the receptor phase, flux is independent from the concentration in the vehicle. Therefore, all test compounds were applied as gel suspensions with an excessive amount of very finely dispersed derivatives relative to the dissolved portion in the donor phase (see Materials and Methods, Diffusion Cell Experiments). In this way continuous saturation of the donor solutions is maintained over the whole period of skin permeation experiments and the perme-

ated amounts of derivatives could be compared, irrespective of their different solubilities in the donor phase.

Furthermore, if rapid solution into the receptor phase is guaranteed, maximum release of the test compounds from the donor phase is obtained, so that a consistent concentration gradient is maintained. Therefore we used a donor phase without buffer capacity to avoid significant dissociation of acidic compounds (**01–03**), but a buffered receptor phase (pH 7.2) to imitate physiological conditions and to produce better solubility *via* increasing dissociation of acids. Maximal flux values, obtained with this permeation model, are summarized as log J_{max} in Table I covering a spectrum of nearly 5 units from the lead **01** to compound **19**. Relatively high flux values are achieved with the amides **06, 05**, and **04**, while the rather lipophilic esters **19** and **18** showed very poor permeation rates.

The experimental results were disappointing with regard to identifying a prodrug that gave better percutaneous absorption as none of the test compounds showed a higher flux in comparison with the parent compound naproxen. Because the new derivatives were not suitable as prodrugs, no experiments were carried out to investigate their enzymatic hydrolysis. However, compounds **08** and **09** are described to be hydrolyzed very quickly in human plasma with known half-lives of 0.6 and 1.4 minutes, respectively (13).

On the other hand, the broad range of log J_{max} data was an important prerequisite to derive significant structure-permeation relationships. The statistical tool we used was PLS-analysis to interpret the skin permeation behavior of the described naproxen derivatives in terms of their physicochemical properties. Beyond calculated lipophilicity (log P) and the solubilities in water (log C_w) and octanol (log C_o), listed in Table I, we used 53 further physicochemical descriptors, which were computed from the 3D-interaction energy maps produced by GRID (17) and transformed by VolSurf (18); for details see methods. The physicochemical descriptors, derived in this way, are detailed in Table II.

One of the general advantages of PLS-analysis is that huge numbers of descriptors (in this example 56) can be applied to comparably low numbers of compounds (in this example 22); results obtained do not depend on the number of descriptors included in the study. From PLS-analysis it can be derived that 88 % of the variance in permeation data can be explained with a three-component model. Components represent combinations of the original descriptors and thereby reduce the dimensionality of the descriptor matrix. In Fig. 1 experimental log J_{max} is plotted against the corresponding recalculated data. In PLS-analysis recalculated Y-data for each compound in the dataset are obtained from the X-data vector of each compound by insertion into the PLS equation model in the following sequence: $X \rightarrow T \rightarrow U \rightarrow Y$. Details of the PLS algorithm are reported elsewhere (27).

The coefficient plot (Fig. 2) expresses the individual contribution of all physicochemical descriptors included in the study by vertical bars. Large bars indicate an important and small bars a negligible contribution; positive directions represent a positive and negative ones an inverse correlation. The plot in Fig. 2 allows the conclusion, that skin permeation

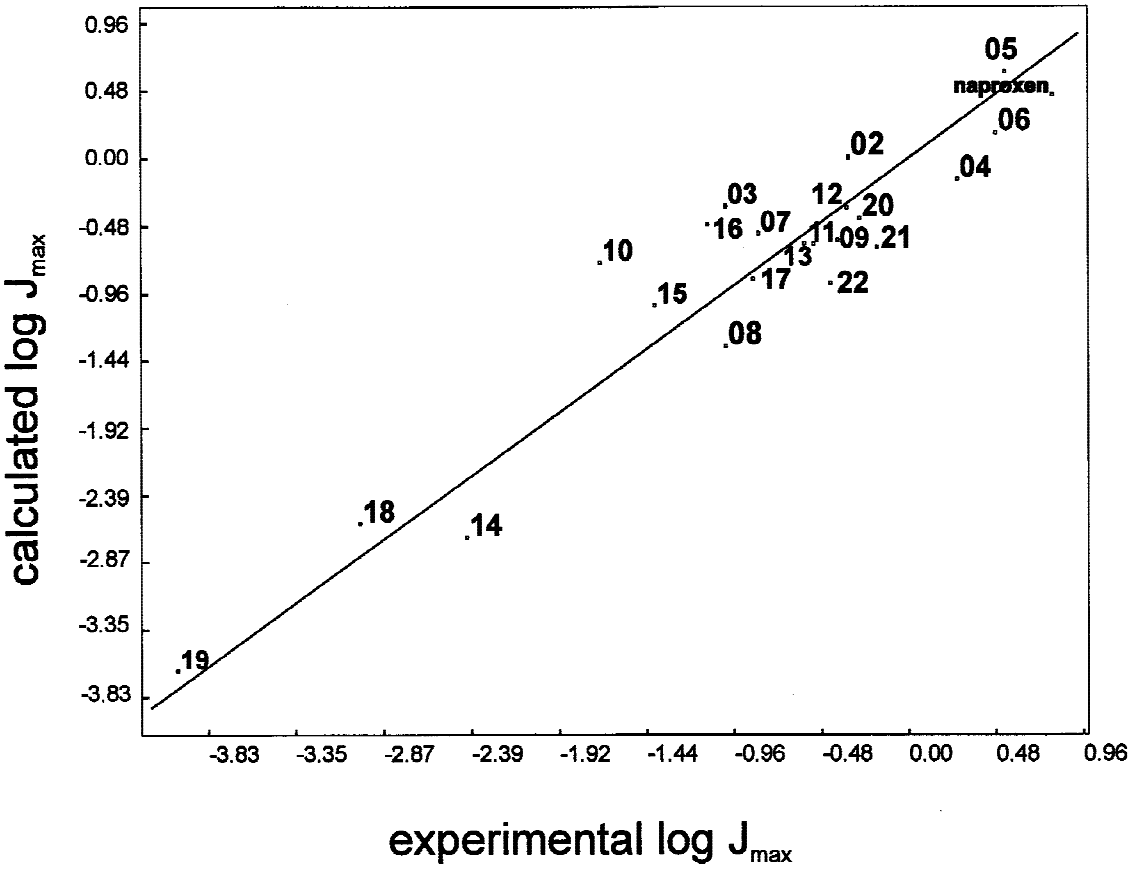

Fig. 1. Plot of experimental skin permeation data (log J_{max}) versus the corresponding calculated data.

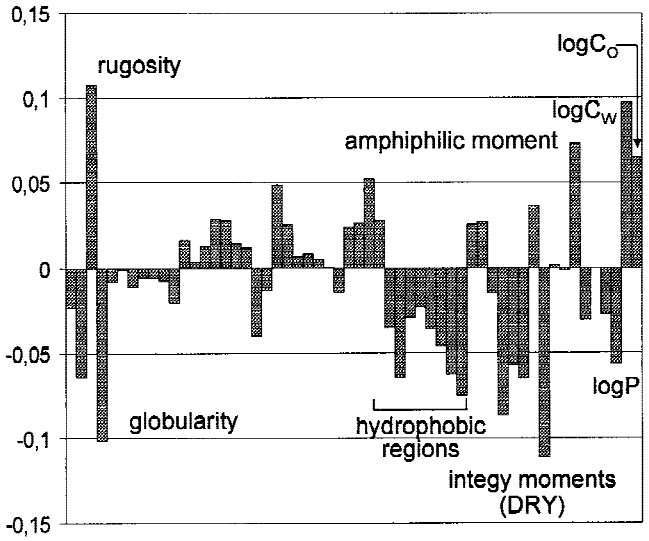

Fig. 2. Coefficient plot expressing the individual contribution of physicochemical descriptors: large bars indicate an important and small bars a slight contribution, positive directions represent a positive and negative ones an inverse correlation. The meaning of the bars— from the left to the right—is identical to the sequence of the VolSurf descriptors listed in Table II: e.g., rugosity (nr 3), globularity (nr 4), hydrophobic regions (nrs 32-39) hydrophobic integy moments (nrs 40-47), and amphiphilic moment (nr 50). Additionally, log P (nr 54), log C_w (nr 55), and log C_O (nr 56) are given.

of naproxen and its derivatives increases with the solubility both in water ($logC_w$) and octanol ($logC_o$), with a large amphiphilic moment and with a high rugosity. The amphiphilic moment is defined as a vector pointing from the centre of the hydrophobic domain to the centre of the hydrophilic domain. The vector length is proportional to the strength of the amphiphilic moment. Thus, the better the separation between the hydrophobic and the hydrophilic domain within a naproxen derivative, the better are its skin permeating properties. The rugosity expresses the ratio of volume to surface and is a measure of the molecular wrinkled surface; the smaller the ratio, the larger is the rugosity. Correspondingly, skin permation increases, when the solvent accessible surface area of the test compound is enlarged.

Inverse correlations are most significant for globularity and integy moments of the DRY probe. Globularity describes the spherical shape of a molecule; globularity is 1.0 in the case of an ideal sphere. Increasing values reflect an increasing deviation from a spherical shape. The inverse correlation of skin permeation with globularity indicates that permeation increases the more spherical the test molecule. Integy moments of the DRY probe measure the unbalance between the center of mass of a molecule and the barycenter of the hydrophobic regions. When integy moments of the DRY probe are high, there is a clear concentration of hydrophobic regions in only one part of the molecular surface. Such a clear concentration of hydrophobic regions is detrimental for skin permeation. Last, but not least high log P values are inversely correlated with skin permeation for this series of naproxen derivatives. The following equation describes the above results:

$$\log J_{max} = 5.22\ R - 2.35\ G - 0.003\ ID8 + 0.04\ A - 0.19\ logP + 0.25 \log C_w + 0.39 \log C_O - 4.39 \quad (2)$$

Beyond interpretation of the data, robustness of the obtained model can be evaluated using cross-validation. It works by building reduced models (one compound removed) and using them to calculate the Y-variable of the compound held out. Then the Y-calculated is compared with the Y-experimental and a correlation coefficient (q) for internal predictivity can be computed, which amounts to 0.67 in the present study. While a direct comparison of the present model with literature data necessitates identical assay conditions, inspection of other hairless mice *in vitro* results (28,29) indicates a nice similarity to our results, showing solubilities both in water and in octanol are important. PLS-analysis, however, is a suitable tool to select those descriptors with highest importance for skin permeation.

PLS-analysis yields a highly significant quantitative model for structure-permeation relationships of naproxen derivatives with a robust internal predictivity. Extension to a larger, chemically more diverse data set would even allow external predictions.

REFERENCES

1. H. Suh, H. W. Jun, M. T. Dzimanski, and G. Lu. Pharmacokinetic and local tissue disposition studies of naproxen following topical and systemic administration in dogs and rats. *Biopharm. Drug Disp.* **18**:623–633 (1997).
2. P. Singh and M. S. Roberts. Skin permeability and local tissue concentrations of nonsteroidal antiinflammatory drugs after topical application. *J. Pharmacol. Exp. Ther.* **268**:144–151 (1994).
3. T. Yano, M. Nakagawa, M. Tsuji, and K. Noda. Skin permeability of various nonsteroidal antiinflammatory drugs in man. *Life Sci.*. **39**:1043–1050 (1986).
4. F. A. van den Ouweland, P. C. Eenhoorn, Y. Tan, and F. W. J. Gribnau. Transcutaneous absorption of naproxen gel. *Eur. J. Clin. Pharmacol.* **36**:209–211 (1989).
5. K. B. Sloan. Functional group consideration in the development of prodrug approaches to solving topical delivery problems. In K. B. Sloan (ed.), *Prodrugs: Topical and Ocular Drug Delivery,* Marcel Dekker, New York, 1992 pp. 17–116.
6. G. B. Kasting, R. L. Smith, and P. D. Anderson. Prodrugs for dermal delivery: Solubility, molecular size, and functional group effects. In K. B. Sloan (ed.), *Prodrugs: Topical and Ocular Drug Delivery,* Marcel Dekker, New York, 1992 pp. 117–161.
7. H. Weber and K. Meyer-Trümpener. Esters of naproxen as prodrugs for skin penetration, I: Synthesis and physicochemical properties. *Arch. Pharm. (Weinheim)* **327**:337–345 (1994).
8. H. Weber, K. Meyer-Trümpener, and B. C. Lippold. Esters of naproxen as prodrugs for skin penetration, II: Penetration behaviour upon excised skin of nude mice. *Arch. Pharm. (Weinheim)* **327**:681–686 (1994).
9. F. P. Bonina, L. Montenegro, and F. Guerrera. Naproxen 1-alkylazacycloalkan-2-one esters as dermal pro-drugs: *In vitro* evaluation. *Int. J. Pharm.* **100**:99–105 (1993).
10. J. Rautio, H. Taipale, J. Gynther, J. Vepsäläinen, T. Nevalainen, and T. Järvinen. *In vitro* evaluation of acyloxyalkyl esters as dermal prodrugs of ketoprofen and naproxen. *J. Pharm. Sci.* **87**: 1622–1628 (1998).
11. J. Rautio, T. Nevalainen, H. Taipale, J. Vepsäläinen, J. Gynther, T. Pedersen, and T. Järvinen. Synthesis and *in vitro* evaluation of aminoacyloxyalkyl esters of 2-(6-methoxy-2-naphthyl)propionic acid as novel naproxen prodrugs for dermal drug delivery. *Pharm. Res.* **16**:1172–1178 (1999).
12. E. Vedejs and N. Lee. Lewis acid induced internal proton return: Enantio-controlled protonation of an amide enolate. *J. Am. Chem. Soc.* **113**:5483–5485 (1991).
13. H. Bundgaard and N. M. Nielsen. Glycolamide esters as a novel biolabile prodrug type for non-steroidal anti-inflammatory carboxylic acid drugs. *Int. J. Pharm.* **43**:101–110 (1988).
14. V. R. Shanbhag, A. M. Crider, R. Gokhale, A. Harpalani, and R. M. Dick. Ester and amide prodrugs of ibuprofen and naproxen:

Synthesis, anti-inflammatory activity, and gastrointestinal toxicity. *J. Pharm. Sci*. **81**:149–154 (1992).
15. J. V. Anderson and S. H. Hansen. Simultaneous quantitative determination of naproxen, its metabolite 6-O-desmethylnaproxen and their five conjugates in plasma and urine samples by high-performance liquid chromatography on dynamically modified silica. *J. Chromatogr*. **577**:325–333 (1992).
16. W. M. Meylan and P. H. Howard. Atom/fragment contribution method for estimating octanol-water partition coefficients. *J. Pharm. Sci*. **84**:83–92 (1995).
17. P. Goodford. A computational procedure for determining energetically favorable binding sites on important macromolecules. *J. Med. Chem.* **28**:849–857 (1985).
18. G. Cruciani, P. Crivori, P.-A. Carrupt, and B. Testa. Molecular fields in quantitative structure-permeation relationships: The VolSurf approach. *J. Molec. Struc.: Theo. Chem*. **503**:17–30 (2000).
19. S. Wold, K. Esbensen, and P. Geladi. Principal component analysis. *Chem. Intell. Lab. System* **2**:37–52 (1987).
20. M. Baroni, G. Costantino, G. Cruciani, D. Riganelli, R. Valigi, and S. Clementi. Generating optimal linear PLS estimations (GOLPE): An advanced chemometric tool for handling 3D-QSAR problems. *Quant. Struct.-Act. Relat*. **12**:9–20 (1993).
21. A.-H. Ghanem, H. Mahmoud, W. I. Higuchi, P. Liu, and W. R. Good. The effects of ethanol on the transport of lipophilic and polar permeants across hairless mouse skin: Methods/validation of a novel approach. *Int. J. Pharm*. **78**:137–156 (1992).
22. Y. Kim, A.-H. Ghanem, H. Mahmoud, and W. I. Higuchi. Short chain alkanols as transport enhancers for lipophilic and polar/ionic permeants in hairless mouse skin: Mechanism(s) of action. *Int. J. Pharm*. **80**:17–31 (1992).
23. T. Hatanaka, K. Katayama, T. Koizumi, K. Sugibayashi, and Y. Morimoto. Time-dependent percutaneous absorption enhancing effect of ethanol. *J. Control. Release* **33**:423–428 (1995).
24. A.-H. Ghanem, H. Mahmoud, W. I. Higuchi, U. D. Rohr, S. Borsadia, P. Liu, J. L. Fox, and W. R. Good. The effects of ethanol on the transport of β-estradiol and other permeants in hairless mouse skin. II. A new quantitative approach. *J. Control. Release* **6**:75–83 (1987).
25. N. A. Megrab, A. C. Williams, and B. W. Barry. Oestradiol permeation across human skin, silastic and snake skin membranes: The effects of ethanol/water co-solvent systems. *Int. J. Pharm*. **116**:101–112 (1995).
26. U. Küpperfahrenberg. Ph D Thesis, Heinrich-Heine-Universität Düsseldorf 1997
27. G. Cruciani and K. Watson. CoMFA using GRID force field and GOLPE variable selection methods in a study of glycogen phosphorylase b. *J. Med. Chem*. **37**:2589–2601 (1994).
28. H. E. Taylor and K. B. Sloan. 1-Alkylcarbonyloxymethyl prodrugs of 5-fluorouracil (5-FU): Synthesis, physicochemical properties and topical delivery of 5-FU. *J. Pharm. Sci*. **87**:15–20 (1998).
29. W. J. Roberts and K. B. Sloan. Correlation of aqueous and lipid solubilities with flux for prodrugs of 5-fluorouracil, theophylline, and 6-mercaptopurine: A Potts-Guy approach. *J. Pharm. Sci*. **88**: 515–522 (1999).